ISET Journal of Earthquake Technology, Paper No. 482, Vol. 44, No. 1, March 2007, pp. 193–211

AN EARTHQUAKE RESPONSE SPECTRUM METHOD FOR LINEAR LIGHT SECONDARY SUBSTRUCTURES

Giuseppe Muscolino and Alessandro Palmeri
Department of Civil Engineering
University of Messina
Vill. S. Agata, 98166, Messina, Italy

ABSTRACT

Earthquake response spectrum is the most popular tool in the seismic analysis and design of structures. In the case of combined primary-secondary (P-S) systems, the response of the supporting P substructure is generally evaluated without considering the S substructure, which in turn is only required to bear displacements and/or forces imposed by the P substructure ("cascade" approach). In doing so, however, dynamic interaction between the P and S components is neglected, and the seismic-induced response of the S substructure may be heavily underestimated or overestimated. In this paper, a novel CQC (Complete Quadratic Combination) rule is proposed for the seismic response of linear light S substructures attached to linear P substructures. The proposed technique overcomes the drawbacks of the cascade approach by including the effects of dynamic interaction and different damping in the substructures directly in the cross-correlation coefficients. The computational effort is reduced by using the eigenproperties of the decoupled substructures and only one earthquake response spectrum for a reference value of the damping ratio.

KEYWORDS: CQC (Complete Quadratic Combination) Rule, Earthquake Response Spectrum, Light Secondary Substructures, Non-classically Damped Structures, Non-structural Components

INTRODUCTION

Although light secondary (S) attachments to buildings or industrial facilities are not part of the primary (P) load-bearing structural system, their seismic analysis and design is a topic of broad engineering interest (among others, Chen and Soong, 1988; Singh, 1988; Villaverde, 2004; Singh et al., 2006a, 2006b; and references provided therein). Past experiences, in fact, prove that S substructures such as suspended ceilings and non-structural walls, piping systems and antennas, storage tanks and electrical transformers must survive earthquakes in order to facilitate emergency and recovery services in the aftermath and avoid direct and/or indirect human and/or economical losses. On the other hand, some special dynamic properties make S substructures particularly vulnerable to earthquakes. First of all, S substructures are usually much lighter than the P substructure to which they are attached, and the stiffness of S components, including anchors, is much smaller than the stiffness of P components: as a result, in most of the real cases the modal frequencies of S substructures are close to, and sometimes tuned to, those of the P substructure. Moreover, the vibration of the P substructure tends to amplify the effects of the ground motion on the S substructures, principally on those attached at the top (e.g., antennas). In addition, the damping capabilities of S attachments are generally much smaller than those of the P supporting system, and so the resonance phenomenon may occur.

The above considerations would suggest the use of rigorous approaches, in which the dynamic interaction among P and S substructures is fully accounted for. In practical applications, however, combined P-S systems have an excessive number of degrees of freedom and show large differences in the mass, stiffness and damping coefficients. Therefore, conventional methods, such as modal analysis with the earthquake response spectrum and time-history analysis with recorded and/or generated accelerograms, may become too expensive and inaccurate. Conversely, the so-called "cascade" approximation, in which feedback of the S substructures on the P substructure is neglected, may be too simplistic even though it is very popular. In this approach, P and S substructures are decoupled and analysed in sequence (e.g., Falsone et al., 1991; Lavelle et al., 1991): in the first stage, the seismic response of the P substructure is evaluated neglecting the presence of any S substructure; in the second

stage, the dynamic response of each S substructure is evaluated considering the motion of the P substructure at the anchor points, other than the ground motion. Unfortunately, in a number of real cases this approach may lead to inaccurate predictions, e.g., when the effect of spatial coupling is significant.

In this paper, the concept of "Light Secondary Substructure" (LSS) approximation is stressed, and the limits of validity are investigated with reference to a simple 2-DOF combined P-S system. This approximation is used in deriving a novel CQC (Complete Quadratic Combination) rule, which can be viewed as a special variant of the method recently formulated by Falsone and Muscolino (1999, 2004) for the seismic analysis of non-classically damped structures. For the validation purposes, numerical results are presented in the simplest case where the new combination coefficients are consistent with the assumption of white noise excitation, while the formulation can be easily extended to any power spectral density (PSD) function of the seismic input. Advantages of the proposed approach are: (i) the eigenproperties involved in the computations (modal frequencies and modal shapes) are those of the decoupled substructures, assumed to be fixed to their own bases; (ii) the cross-correlation coefficients incorporate the effects of frequency tuning and different damping in the substructures; and (iii) just a single earthquake response spectrum, for a reference value of the viscous damping ratio, is required. The latter feature of the proposed approach is probably the most important one. Methods based on the direct characterization of the seismic hazard by the PSD of the ground acceleration, in fact, enable to account for the dynamic interaction among P and S substructures through the appropriate definition of the frequency response function (FRF) of the combined P-S system, for which the individual fixed-base modal properties can be used (Dey and Gupta, 1999). However, to date, the PSD function is considered almost exclusively in the academic community and for studying structures of exceptional importance. Seventy-five years after the pioneering work by Professor Maurice Biot (Biot, 1932, 1933, 1934), the earthquake response spectrum is still the most popular tool for the analysis and design of conventional earthquake-resistant structures. Moreover, given its extreme simplicity, a number of deterministic and stochastic extensions have been proposed in the literature. Among others, Amini and Trifunac (1985) developed a stochastic method for estimating not just the largest, but all the ordered peaks of the seismic response of linear structures; this method has been refined by Gupta and Trifunac (1988), and can be useful in order to better understand the progressive damage under successive excursions of the seismic response beyond a certain design level; Gupta and Trifunac (1989) formulated a probabilistic extension, which takes into account the rotational components of the ground motion along with the translational components; the effects of wave passage, loss of coherency with distance and variation of local soil conditions are included in the method proposed by Der Kiureghian and Neuenhofer (1992) for the seismic analysis of multiply-supported structures subjected to spatially-varying ground motions; Iwan (1997) proposed a new earthquake drift spectrum based on a continuous shear-beam model rather than a single-degree-of-freedom oscillator, which provides important information for near-source pulse-like ground shakings. From this point of view, then, the main intent of the CQC rule proposed in this paper could be claimed to be the attempt of extending to light secondary attachments the original statement by Professor Maurice Biot: "the maximum effect of earthquakes on buildings will be easily evaluated…" (Biot, 1933).

EQUATIONS OF MOTION

In this section, the equations of motion of a primary (P) structural system with n_P DOFs (degrees of freedom), connected to a lighter secondary (S) attachment with n_S DOFs, are established in the linear range. In the following, the damping of both P and S substructures is assumed to be linear hysteretic (among others, Nashif et al., 1985; Inaudi and Kelly, 1995; Muscolino et al., 2005; and references provided therein). Experimental analyses, in fact, demonstrate that in most of the cases the dissipation of engineering materials is nearly frequency-independent. This means that, ideally, the damping forces are proportional to the strains, but in phase with the strain rates. This behaviour can be easily introduced in the frequency domain, while much more complicated is the application in the time domain (Makris, 1997; Makris and Zhang, 2000; Muscolino et al., 2005), and for this reason the linear viscous damping is usually preferred in structural dynamics. However, when combined P-S systems are dealt with, the formation of the viscous damping matrix is not straightforward (e.g., Gupta and Jaw, 1986; Muscolino, 1990; Feriani and Perotti, 1996), and the use of the linear hysteretic damping is preferable.

1. Combined P-S System

In the mixed time-frequency domain, the seismic motion of the combined P-S system shown in Figure 1 is governed by

$$\mathbf{M}\ddot{\mathbf{u}}(t)+\mathbf{K}(\omega)\mathbf{u}(t)=-\mathbf{M}\boldsymbol{\tau}\ddot{u}_{\mathrm{g}}(t) \tag{1}$$

Here $\mathbf{u}(t)=\left[\mathbf{u}_{\mathrm{S}}^{T}(t)\ \vdots\ \mathbf{u}_{\mathrm{P}}^{T}(t)\right]^{T}$ is the $n\times 1$ array ($n=n_{\mathrm{S}}+n_{\mathrm{P}}$) of the DOFs (total displacements), in which those of the P substructure, as listed in the array $\mathbf{u}_{\mathrm{P}}(t)$, are appended to the DOFs of the S substructure, as listed in the array $\mathbf{u}_{\mathrm{S}}(t)$; $\ddot{u}_{\mathrm{g}}(t)$ is the time history of the ground acceleration; $\boldsymbol{\tau}$ is its influence vector whose elements can be partitioned as $\boldsymbol{\tau}=\left[\boldsymbol{\tau}_{\mathrm{S}}^{T}\ \vdots\ \boldsymbol{\tau}_{\mathrm{P}}^{T}\right]^{T}$; $\mathbf{M}$ and $\mathbf{K}(\omega)$ are the inertia matrix and the complex-valued dynamic stiffness matrix, respectively; and, as usual, the over-dot means time derivative. The matrices $\mathbf{M}$ and $\mathbf{K}(\omega)$ can be partitioned as

$$\begin{aligned}\mathbf{M}&=\left[\begin{array}{c:c}\mathbf{M}_{\mathrm{S}} & \mathbf{0}\\ \hdashline \mathbf{0} & \mathbf{M}_{\mathrm{P}}\end{array}\right]\\ \mathbf{K}(\omega)&=\left[\begin{array}{c:c}\mathbf{K}_{\mathrm{S}}\times\left[1+\mathrm{j}\,\eta_{\mathrm{S}}\,\mathrm{sign}(\omega)\right] & \mathbf{0}\\ \hdashline \mathbf{0} & \mathbf{K}_{\mathrm{P}}\times\left[1+\mathrm{j}\,\eta_{\mathrm{P}}\,\mathrm{sign}(\omega)\right]\end{array}\right]+\left[\begin{array}{c:c}\mathbf{0} & \mathbf{K}_{\mathrm{SP}}\\ \hdashline \mathbf{K}_{\mathrm{SP}}^{\mathrm{T}} & \Delta\mathbf{K}_{\mathrm{P}}\end{array}\right]\times\left[1+\mathrm{j}\,\eta_{\mathrm{S}}\,\mathrm{sign}(\omega)\right]\end{aligned} \tag{2}$$

Here the real-valued mass and stiffness matrices of the S substructure, $\mathbf{M}_{\mathrm{S}}$ and $\mathbf{K}_{\mathrm{S}}$, and of the P substructure, $\mathbf{M}_{\mathrm{P}}$ and $\mathbf{K}_{\mathrm{P}}$, refer to the substructures assembled under the assumption of being fixed to their respective bases, i.e., the P substructure is fixed to the ground (Figure 2(a)), while the S substructure is fixed to the support points on the P substructure as well as to the ground (Figure 2(b)); $\mathbf{K}_{\mathrm{SP}}$ is the stiffness matrix coupling the P and S substructures; $\Delta\mathbf{K}_{\mathrm{P}}$ is the increment in the stiffness matrix of the P substructure due to the presence of the S substructure; η_{S} and η_{P} are the loss factors of the S and P substructures, respectively; $\mathrm{j}=\sqrt{-1}$ is the imaginary unit; and ω is the vibration frequency.

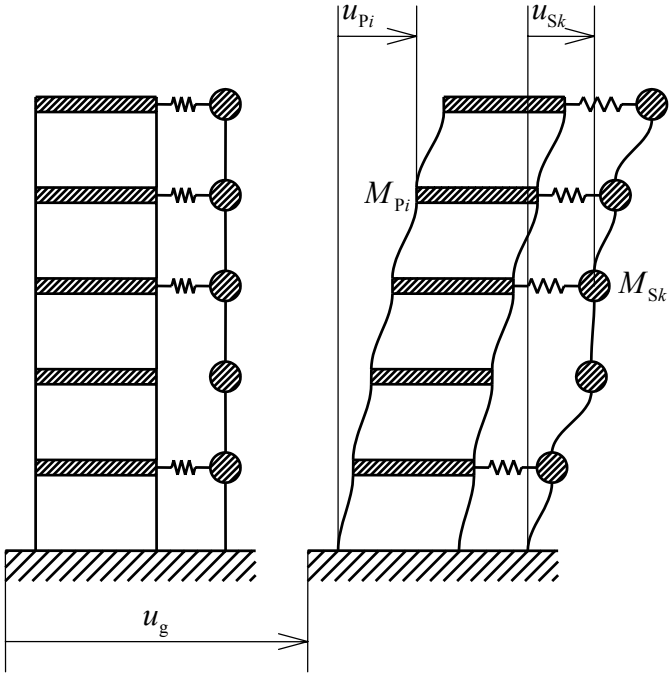

Fig. 1 Sketch of the combined primary-secondary (P-S) system

The seismic response of the coupled P-S system is given in the frequency domain by

$$\mathrm{F}\left\langle \mathbf{u}(t)\right\rangle = \mathbf{H}(\omega)\,\mathrm{F}\left\langle \ddot{u}_{\mathrm{g}}(t)\right\rangle \tag{3}$$

where the symbol $\mathrm{F}\langle\cdot\rangle$ stands for the Fourier transform operator, and $\mathbf{H}(\omega)$ is the $n\times 1$ array listing the frequency response functions (FRFs) of various DOFs:

$$\mathbf{H}(\omega) = -\left[\mathbf{M}^{-1}\mathbf{K}(\omega) - \omega^2\mathbf{I}_n\right]^{-1}\boldsymbol{\tau} \tag{4}$$

with $\mathbf{I}_n$ being the $n\times n$ identity matrix.

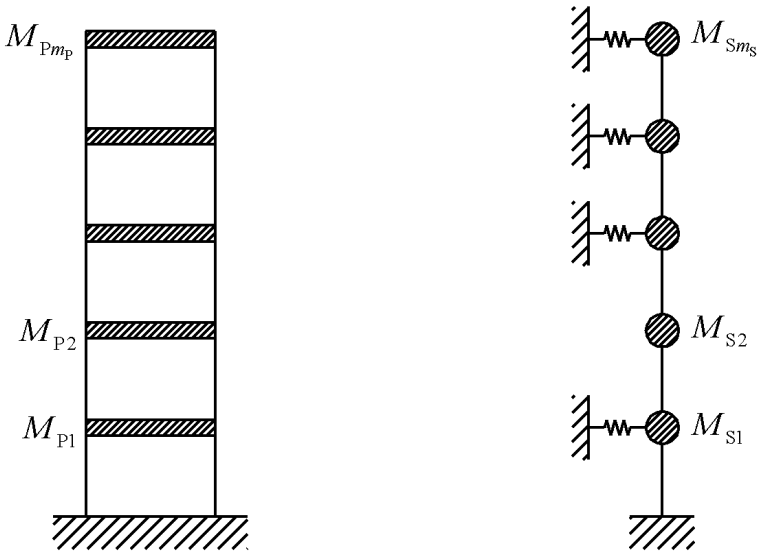

Fig. 2 Fixed-base substructures: (a) P structural system; (b) S attachment

2. Modal Transformations

The dynamic response of the combined P-S system can be conveniently represented in the reduced modal space by means of the so-called "admissible coordinate transformation" (Muscolino, 1990), given by

$$\mathbf{u}(t) = \boldsymbol{\Gamma}\mathbf{q}(t) \tag{5}$$

Here $\mathbf{q}(t) = \left[\mathbf{q}_{\mathrm{S}}^T(t) \;\vdots\; \mathbf{q}_{\mathrm{P}}^T(t)\right]^T$ is the $m\times 1$ array ($m = m_{\mathrm{S}} + m_{\mathrm{P}} \le n$) listing the modal coordinates of the combined P-S system, in which the array of the $m_{\mathrm{P}} \le n_{\mathrm{P}}$ modal coordinates of the P substructure, $\mathbf{q}_{\mathrm{P}}(t)$, is appended to the array of the $m_{\mathrm{S}} \le n_{\mathrm{S}}$ modal coordinates of the S substructure, $\mathbf{q}_{\mathrm{S}}(t)$; and $\boldsymbol{\Gamma}$ is the transformation matrix, which is partitioned as

$$\boldsymbol{\Gamma} = \left[\begin{array}{c:c} \boldsymbol{\Phi}_{\mathrm{S}} & \boldsymbol{\Psi}_{\mathrm{SP}} \\ \hdashline \mathbf{0} & \boldsymbol{\Phi}_{\mathrm{P}} \end{array}\right] \tag{6}$$

with $\boldsymbol{\Phi}_{\mathrm{S}} = \left[\boldsymbol{\phi}_{\mathrm{S}1} \;\cdots\; \boldsymbol{\phi}_{\mathrm{S}m_{\mathrm{S}}}\right]$ and $\boldsymbol{\Phi}_{\mathrm{P}} = \left[\boldsymbol{\phi}_{\mathrm{P}1} \;\cdots\; \boldsymbol{\phi}_{\mathrm{P}m_{\mathrm{P}}}\right]$ being the modal matrices of the S and P substructures, of dimensions $n_{\mathrm{S}}\times m_{\mathrm{S}}$ and $n_{\mathrm{P}}\times m_{\mathrm{P}}$, respectively. The columns of these matrices are the modal shapes of the two fixed-base substructures (Figures 3(a) and 3(b)). In Equation (6), $\boldsymbol{\Psi}_{\mathrm{SP}} = \left[\boldsymbol{\psi}_{\mathrm{SP}1} \;\cdots\; \boldsymbol{\psi}_{\mathrm{SP}m_{\mathrm{S}}}\right]$ is the modal coupling matrix, of dimensions $n_{\mathrm{S}}\times m_{\mathrm{P}}$, whose columns are the deformed shapes of the S substructure due to the displacements at the support points for the modal shapes of the P substructure (Figure 3(c)). The modal matrices $\boldsymbol{\Phi}_{\mathrm{S}}$ and $\boldsymbol{\Phi}_{\mathrm{P}}$ can be evaluated by solving the following classical eigenproblems:

$$\mathbf{M}_{\mathrm{S}}\boldsymbol{\Phi}_{\mathrm{S}}\boldsymbol{\Omega}_{\mathrm{S}}^{2}=\mathbf{K}_{\mathrm{S}}\boldsymbol{\Phi}_{\mathrm{S}};\quad \mathbf{M}_{\mathrm{P}}\boldsymbol{\Phi}_{\mathrm{P}}\boldsymbol{\Omega}_{\mathrm{P}}^{2}=\mathbf{K}_{\mathrm{P}}\boldsymbol{\Phi}_{\mathrm{P}} \tag{7}$$

$\boldsymbol{\Omega}_{\mathrm{S}}=\mathrm{diag}\left\{\omega_{\mathrm{S}1},\cdots,\omega_{\mathrm{S}m_{\mathrm{S}}}\right\}$ and $\boldsymbol{\Omega}_{\mathrm{P}}=\mathrm{diag}\left\{\omega_{\mathrm{P}1},\cdots,\omega_{\mathrm{P}m_{\mathrm{P}}}\right\}$ being the spectral matrices of the S and P substructures, respectively. The elements of these matrices are the undamped modal circular frequencies of the two fixed-base substructures. Further, the modal coupling matrix $\boldsymbol{\Psi}_{\mathrm{SP}}$ is given by

$$\boldsymbol{\Psi}_{\mathrm{SP}}=\mathbf{N}_{\mathrm{SP}}\boldsymbol{\Phi}_{\mathrm{P}};\quad \mathbf{N}_{\mathrm{SP}}=-\mathbf{K}_{\mathrm{S}}^{-1}\mathbf{K}_{\mathrm{SP}} \tag{8}$$

with $\mathbf{N}_{\mathrm{SP}}$ being the so-called pseudo-static influence matrix of the P substructure on the S substructure.

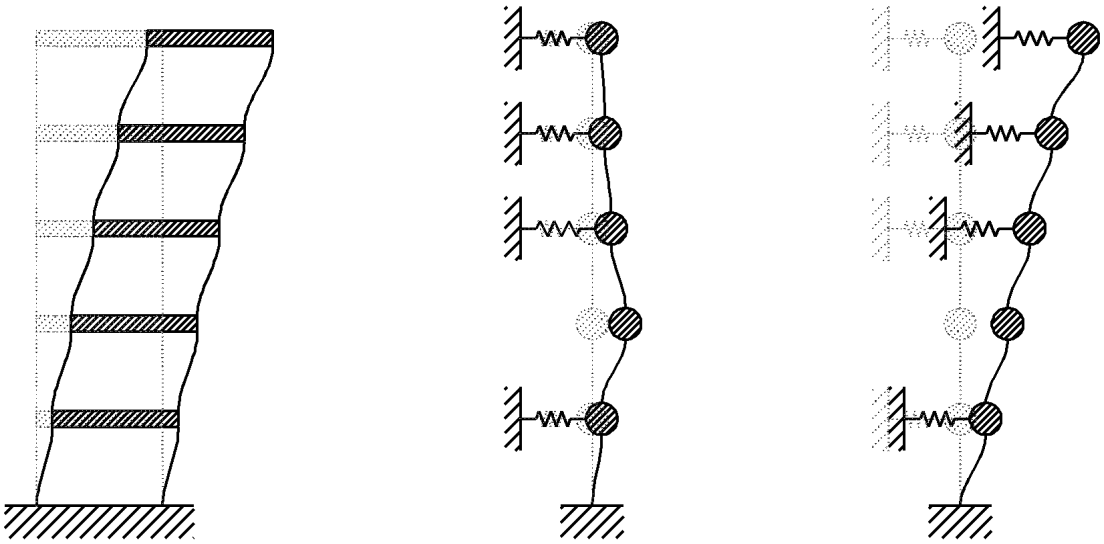

(a) (b) (c)

Fig. 3 (a) Modal shape of the P structural system; (b) Modal shape of the fixed-base S attachment; (c) Deformed shape of the S attachment induced by the modal shape of the P structural system

Upon substitution of Equation (5) into Equation (1), one obtains

$$\mathbf{m}\ddot{\mathbf{q}}(t)+\mathbf{k}(\omega)\mathbf{q}(t)=\mathbf{g}\ddot{u}_{\mathrm{g}}(t) \tag{9}$$

where the symmetric matrices $\mathbf{m}$ and $\mathbf{k}(\omega)$ are the inertia matrix and the complex-valued dynamic stiffness matrix in the reduced modal space, respectively, while $\mathbf{g}$ is the modal influence vector of the seismic input. These quantities are expressed as

$$\mathbf{m}=\boldsymbol{\Gamma}^{T}\mathbf{M}\boldsymbol{\Gamma}=\left[\begin{array}{c|c}\mathbf{I}_{m_{\mathrm{S}}} & \mathbf{m}_{\mathrm{SP}}\\ \hline \mathbf{m}_{\mathrm{SP}}^{\mathrm{T}} & \mathbf{I}_{m_{\mathrm{P}}}+\Delta\mathbf{m}_{\mathrm{P}}\end{array}\right]$$

$$\mathbf{k}(\omega)=\boldsymbol{\Gamma}^{T}\mathbf{K}(\omega)\boldsymbol{\Gamma}=\left[\begin{array}{c|c}\boldsymbol{\Omega}_{\mathrm{S}}^{2}\gamma(\omega) & \mathbf{0}\\ \hline \mathbf{0} & \boldsymbol{\Omega}_{\mathrm{P}}^{2}+\Delta\mathbf{k}_{\mathrm{P}}\gamma(\omega)\end{array}\right]\times\left[1+\mathrm{j}\,\eta_{\mathrm{P}}\,\mathrm{sign}(\omega)\right] \tag{10}$$

$$\mathbf{g}=-\boldsymbol{\Gamma}^{T}\mathbf{M}\boldsymbol{\tau}=-\left[\begin{array}{c}\mathbf{p}_{\mathrm{S}}\\ \hline \mathbf{p}_{\mathrm{P}}+\Delta\mathbf{p}_{\mathrm{P}}\end{array}\right]$$

where the off-diagonal term $\mathbf{m}_{\mathrm{SP}}$ in the inertia matrix is defined by

$$\mathbf{m}_{\mathrm{SP}}=\boldsymbol{\Phi}_{\mathrm{S}}^{T}\mathbf{M}_{\mathrm{S}}\boldsymbol{\Psi}_{\mathrm{SP}} \tag{11}$$

and $\mathbf{p}_{\mathrm{S}}$ and $\mathbf{p}_{\mathrm{P}}$ are the arrays listing the usual modal participation factors of the P and S substructures, respectively:

$$\mathbf{p}_{\mathrm{S}} = \boldsymbol{\Phi}_{\mathrm{S}}^{T}\mathbf{M}_{\mathrm{S}}\boldsymbol{\tau}_{\mathrm{S}}; \quad \mathbf{p}_{\mathrm{P}} = \boldsymbol{\Phi}_{\mathrm{P}}^{T}\mathbf{M}_{\mathrm{P}}\boldsymbol{\tau}_{\mathrm{P}} \tag{12}$$

Further, the increments $\Delta\mathbf{m}_{\mathrm{P}}$, $\Delta\mathbf{k}_{\mathrm{P}}$ and $\Delta\mathbf{p}_{\mathrm{P}}$ are given by

$$\begin{gathered}\Delta\mathbf{m}_{\mathrm{P}} = \boldsymbol{\Psi}_{\mathrm{SP}}^{T}\mathbf{M}_{\mathrm{S}}\boldsymbol{\Psi}_{\mathrm{SP}}; \quad \Delta\mathbf{k}_{\mathrm{P}} = \boldsymbol{\Phi}_{\mathrm{P}}^{T}\left(\Delta\mathbf{K}_{\mathrm{P}} + \mathbf{K}_{\mathrm{SP}}^{T}\mathbf{N}_{\mathrm{SP}}\right)\boldsymbol{\Phi}_{\mathrm{P}} \\ \Delta\mathbf{p}_{\mathrm{P}} = \boldsymbol{\Phi}_{\mathrm{P}}^{T}\mathbf{N}_{\mathrm{SP}}^{T}\mathbf{M}_{\mathrm{S}}\boldsymbol{\tau}_{\mathrm{S}}\end{gathered} \tag{13}$$

and $\gamma(\omega)$ is a complex-valued function that accounts for the different damping in the substructures:

$$\gamma(\omega) = \frac{1+\mathrm{j}\,\eta_{\mathrm{S}}\,\mathrm{sign}(\omega)}{1+\mathrm{j}\,\eta_{\mathrm{P}}\,\mathrm{sign}(\omega)} = \frac{(1+\eta_{\mathrm{S}}\eta_{\mathrm{P}})+\mathrm{j}(\eta_{\mathrm{S}}-\eta_{\mathrm{P}})\,\mathrm{sign}(\omega)}{1+\eta_{\mathrm{P}}^{2}} \tag{14}$$

According to Equations (5) and (10), the seismic response of the coupled P-S system can be evaluated in the frequency domain as

$$\mathrm{F}\left\langle\mathbf{u}(t)\right\rangle = \boldsymbol{\Gamma}\mathbf{h}(\omega)\,\mathrm{F}\left\langle\ddot{u}_{\mathrm{g}}(t)\right\rangle \tag{15}$$

where $\mathbf{h}(\omega)$ is the $m\times 1$ array listing the modal FRFs:

$$\mathbf{h}(\omega) = \left[\mathbf{k}(\omega) - \omega^{2}\mathbf{m}\right]^{-1}\mathbf{g} = \left[\mathbf{A}(\omega) - \omega^{2}\mathbf{I}_{m}\right]^{-1}\mathbf{b} \tag{16}$$

with

$$\mathbf{A}(\omega) = \mathbf{m}^{-1}\mathbf{k}(\omega); \quad \mathbf{b} = \mathbf{m}^{-1}\mathbf{g} \tag{17}$$

APPROXIMATE RESPONSE OF A SIMPLE 2-DOF COMBINED P-S SYSTEM

In this section, the simplest case in which both P and S substructures are single-DOF oscillators is considered, with the aim of investigating the effects that two different approximations, namely the "Light Secondary Substructure" (LSS) approximation and the "cascade" approximation, may have on the seismic response of the combined P-S system. This analysis reveals which terms are negligible when the S substructure is much lighter than the P substructure, and these results are extended in the next section to the general case in which both P and S substructures are multi-DOF systems.

With reference to the combined P-S system depicted in Figure 4(a), the matrices $\mathbf{M}$ and $\mathbf{K}(\omega)$ in Equation (2) are simplified as

$$\begin{gathered}\mathbf{M} = \left[\begin{array}{c|c} M_{\mathrm{S}} & 0 \\ \hline 0 & M_{\mathrm{P}} \end{array}\right] \\ \mathbf{K}(\omega) = \left[\begin{array}{c|c} K_{\mathrm{S}}\gamma(\omega) & -\dfrac{K_{\mathrm{S}}}{2}\gamma(\omega) \\ \hline -\dfrac{K_{\mathrm{S}}}{2}\gamma(\omega) & K_{\mathrm{P}} + \dfrac{K_{\mathrm{S}}}{2}\gamma(\omega) \end{array}\right] \times \left[1+\mathrm{j}\,\eta_{\mathrm{P}}\,\mathrm{sign}(\omega)\right]\end{gathered} \tag{18}$$

while $\mathbf{u}(t) = \left[u_{\mathrm{S}}(t) \;\vdots\; u_{\mathrm{P}}(t)\right]^{T}$ and $\boldsymbol{\tau} = \left[1 \;\vdots\; 1\right]^{T}$. After some algebra, one can prove that the transformation matrix $\boldsymbol{\Gamma}$ consistent with Equation (6) is

$$\boldsymbol{\Gamma} = \left[\begin{array}{c|c} M_{\mathrm{S}}^{-1/2} & \dfrac{1}{2}M_{\mathrm{P}}^{-1/2} \\ \hline 0 & M_{\mathrm{P}}^{-1/2} \end{array}\right] \tag{19}$$

The modal quantities in Equation (10) are then expressed as

$$\mathbf{m} = \left[\begin{array}{c|c} 1 & \dfrac{\sqrt{\alpha}}{2} \\ \hline \dfrac{\sqrt{\alpha}}{2} & 1+\dfrac{\alpha}{4} \end{array}\right]; \quad \mathbf{k}(\omega) = \omega_{\mathrm{P}}^2 \times \left[\begin{array}{c|c} \beta^2\gamma(\omega) & 0 \\ \hline 0 & 1+\dfrac{\alpha\,\beta^2\gamma(\omega)}{4} \end{array}\right] \times \left[1 + \mathrm{j}\,\eta_{\mathrm{P}}\,\mathrm{sign}(\omega)\right] \tag{20}$$

$$\mathbf{g} = -\left[\begin{array}{c} \sqrt{\alpha} \\ \hline 1+\dfrac{\alpha}{2} \end{array}\right]$$

where α is the mass ratio and β is a tuning parameter:

$$\alpha = \frac{M_{\mathrm{S}}}{M_{\mathrm{P}}}; \quad \beta = \frac{\omega_{\mathrm{S}}}{\omega_{\mathrm{P}}} \tag{21}$$

ω_{P} and ω_{S} being the undamped natural circular frequencies of the P (Figure 4(b)) and S (Figure 4(c)) oscillators:

$$\omega_{\mathrm{P}} = \sqrt{\frac{K_{\mathrm{P}}}{M_{\mathrm{P}}}}; \quad \omega_{\mathrm{S}} = \sqrt{\frac{K_{\mathrm{S}}}{M_{\mathrm{S}}}} \tag{22}$$

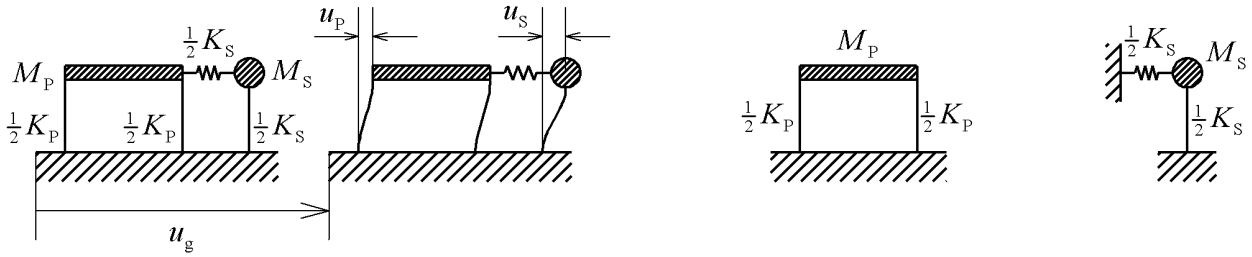

(a) (b) (c)

Fig. 4 (a) 2-DOF combined P-S system; (b) P oscillator; (c) S oscillator

1. LSS Approximation

When the S substructure is light with respect to the P substructure, i.e., $M_{\mathrm{S}} \ll M_{\mathrm{P}}$, the mass ratio (first of Equations (21)) is much less than one, i.e., $\alpha \ll 1$. Accordingly, this term can be neglected in the dynamic stiffness matrix and in the influence vector given in Equations (20):

$$\hat{\mathbf{k}}(\omega) = \omega_{\mathrm{P}}^2 \times \left[\begin{array}{c|c} \beta^2\gamma(\omega) & 0 \\ \hline 0 & 1 \end{array}\right] \times \left[1 + \mathrm{j}\,\eta_{\mathrm{P}}\,\mathrm{sign}(\omega)\right]; \quad \hat{\mathbf{g}} = -\left[\begin{array}{c} \sqrt{\alpha} \\ \hline 1 \end{array}\right] \tag{23}$$

Additionally, in the complex-valued modal stiffness matrix $\hat{\mathbf{k}}(\omega)$ (first of Equations (23)) it is assumed that $\left|\alpha\beta^2\gamma(\omega)\right| \ll 1$. In practical applications, in fact, $\left|\gamma(\omega)\right| \cong 1$, while from Equations (21) and (22) it follows that the stiffness ratio $K_{\mathrm{S}}/K_{\mathrm{P}}$ is given by $\alpha\beta^2$. This ratio needs to be much less than one in order for the "secondary" stiffness K_{S} to be negligible with respect to the "primary" stiffness K_{P}.

Upon substitution of Equation (23) into Equation (17), one obtains for the proposed LSS approximation

$$\hat{\mathbf{A}}(\omega)=\mathbf{m}^{-1}\hat{\mathbf{k}}(\omega)=\omega_{\mathrm{P}}^{2}\times\left[\begin{array}{c|c}\left(1+\dfrac{\alpha}{4}\right)\beta^{2}\gamma(\omega) & -\dfrac{\sqrt{\alpha}}{2}\\ \hline -\dfrac{\sqrt{\alpha}}{2}\beta^{2}\gamma(\omega) & 1\end{array}\right]\times\left[1+\mathrm{j}\,\eta_{\mathrm{P}}\,\mathrm{sign}(\omega)\right]$$

$$\hat{\mathbf{b}}=\mathbf{m}^{-1}\hat{\mathbf{g}}=-\left[\begin{array}{c}\dfrac{\sqrt{\alpha}}{2}+\dfrac{\alpha\sqrt{\alpha}}{4}\\ \hline 1-\dfrac{\alpha}{2}\end{array}\right]\cong-\left[\begin{array}{c}\dfrac{\sqrt{\alpha}}{2}\\ \hline 1\end{array}\right] \tag{24}$$

with

$$\mathbf{m}^{-1}=\left[\begin{array}{c|c}1+\dfrac{\alpha}{4} & -\dfrac{\sqrt{\alpha}}{2}\\ \hline -\dfrac{\sqrt{\alpha}}{2} & 1\end{array}\right] \tag{25}$$

The approximate array of the modal FRFs, then, can be evaluated as

$$\hat{\mathbf{h}}(\omega)=\left[\hat{\mathbf{A}}(\omega)-\omega^{2}\mathbf{I}_{2}\right]^{-1}\hat{\mathbf{b}}=\left[\begin{array}{c}\hat{h}_{\mathrm{S}}(\omega)\\ \hline \hat{h}_{\mathrm{P}}(\omega)\end{array}\right] \tag{26}$$

where $\hat{h}_{\mathrm{S}}(\omega)$ and $\hat{h}_{\mathrm{P}}(\omega)$ are the approximate FRFs of the modal coordinates of the S oscillator, $q_{\mathrm{S}}(t)=\sqrt{M_{\mathrm{S}}}\left[u_{\mathrm{S}}(t)-u_{\mathrm{P}}(t)/2\right]$, and of the P oscillator, $q_{\mathrm{P}}(t)=\sqrt{M_{\mathrm{P}}}u_{\mathrm{P}}(t)$, respectively. The comparison between Equations (3) and (15), finally, gives the array of the corresponding FRFs of the DOFs, $u_{\mathrm{S}}(t)$ and $u_{\mathrm{P}}(t)$, in that order:

$$\hat{\mathbf{H}}(\omega)=\boldsymbol{\Gamma}\hat{\mathbf{h}}(\omega)=\left[\begin{array}{c}M_{\mathrm{S}}^{-1/2}\hat{h}_{\mathrm{S}}(\omega)+\dfrac{1}{2}M_{\mathrm{P}}^{-1/2}\hat{h}_{\mathrm{P}}(\omega)\\ \hline M_{\mathrm{P}}^{-1/2}\hat{h}_{\mathrm{P}}(\omega)\end{array}\right] \tag{27}$$

2. Cascade Approximation

When the S substructure is much lighter than the P substructure, i.e., $\alpha\ll 1$, the dynamic interaction in the coupled P-S system is often ignored, and the seismic responses of the P and S substructures are evaluated in cascade. Accordingly, in the first stage the response of the P substructure to the ground motion is computed by neglecting the feedback of the S substructure, while in the second stage the response of the S substructure is computed by taking into account both the response of the P substructure and the seismic input. As a result, the dynamic stiffness matrix $\mathbf{K}(\omega)$ in the second of Equations (18) becomes asymmetric, since the lower off-diagonal term becomes zero:

$$\bar{\mathbf{K}}(\omega)=\left[\begin{array}{c|c}K_{\mathrm{S}}\left[1+\mathrm{j}\,\eta_{\mathrm{S}}\,\mathrm{sign}(\omega)\right] & -\dfrac{K_{\mathrm{S}}}{2}\left[1+\mathrm{j}\,\eta_{\mathrm{S}}\,\mathrm{sign}(\omega)\right]\\ \hline 0 & K_{\mathrm{P}}\left[1+\mathrm{j}\,\eta_{\mathrm{P}}\,\mathrm{sign}(\omega)\right]\end{array}\right] \tag{28}$$

The approximate array of the FRFs of the DOFs then takes the form

$$\bar{\mathbf{H}}(\omega) = -\left[\mathbf{M}^{-1}\bar{\mathbf{K}}(\omega) - \omega^2\mathbf{I}_n\right]^{-1}\boldsymbol{\tau} = \begin{bmatrix} \dfrac{\omega^2 - \left[1 + \dfrac{\beta^2\gamma(\omega)}{2}\right]\omega_{\mathrm{P}}^2\left[1 + \mathrm{j}\eta_{\mathrm{P}}\,\mathrm{sign}(\omega)\right]}{\left\{\omega^2 - \beta^2\omega_{\mathrm{S}}^2\left[1 + \mathrm{j}\eta_{\mathrm{S}}\,\mathrm{sign}(\omega)\right]\right\}\left\{\omega^2 - \omega_{\mathrm{P}}^2\left[1 + \mathrm{j}\eta_{\mathrm{P}}\,\mathrm{sign}(\omega)\right]\right\}} \\ \dfrac{1}{\omega^2 - \omega_{\mathrm{P}}^2\left[1 + \mathrm{j}\eta_{\mathrm{P}}\,\mathrm{sign}(\omega)\right]} \end{bmatrix} \tag{29}$$

3. Numerical Examples

The accuracy of the approximations summarized in the previous subsections has been investigated in the frequency domain. In Figure 5 the absolute values of the exact FRFs of both P and S substructures (shown by solid lines) are compared with those given by the LSS approximation (as in Equation (27); shown by circles) and cascade approximation (as in Equation (29); shown by dashed lines). The mass ratio and the tuning parameter are $\alpha = 0.02$ and $\beta = 1.0$, respectively, while the loss factors for the P and S substructures are $\eta_{\mathrm{S}} = 0.04$ and $\eta_{\mathrm{P}} = 0.10$. These comparisons demonstrate that the proposed LSS approximation is in good agreement with the exact solution even when the P and S oscillators are perfectly tuned, i.e., $\beta = 1.0$. On the contrary, the cascade approximation is unable to recover the bimodal FRF of the P oscillator (Figure 5, left), and overestimates the peak for the S oscillator (Figure 5, right). The semi-logarithmic plots in Figure 6 confirm the higher accuracy of the proposed LSS approximation (shown by circles) with respect to the classical cascade approximation (shown by dashed line) for a larger mass ratio ($\alpha = 0.10$) and different values of the tuning parameter ($\beta = 0.50$, 1.0 and 1.5). However, only when $\beta = 1.0$, the inaccuracy of the cascade approximation drastically affects the results.

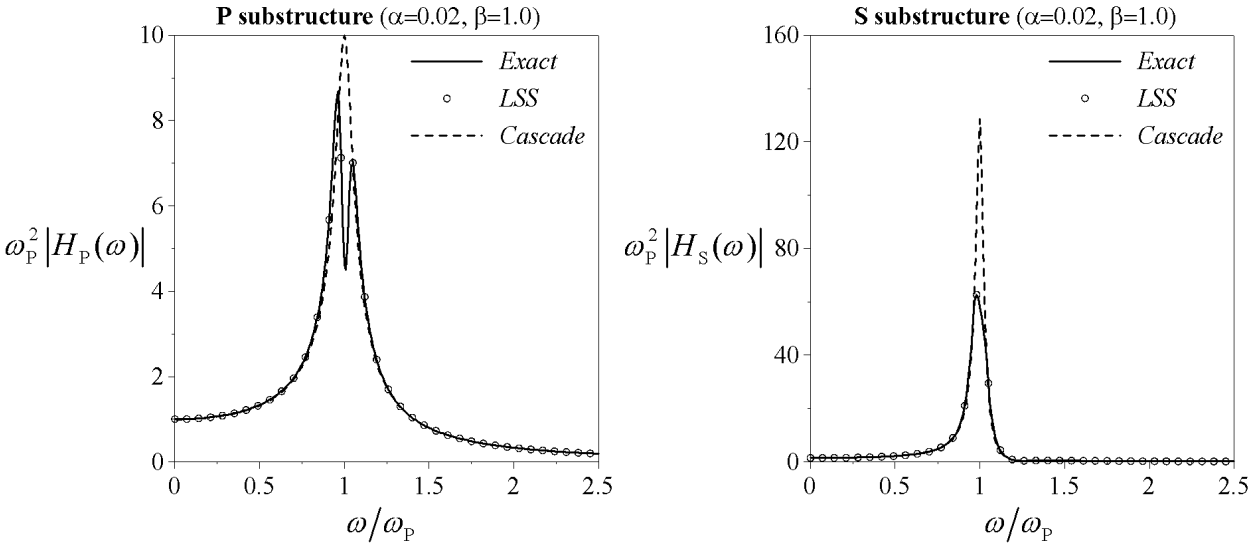

Fig. 5 Dimensionless absolute values of the frequency response functions of the 2-DOF combined P-S system with mass ratio $\alpha = 0.02$ and tuning parameter $\beta = 1.0$: P oscillator (left); S oscillator (right)

APPROXIMATE RESPONSE OF MULTI-DOF COMBINED P-S SYSTEMS

Let us go back to the modal equations of motion of multi-DOF P and S substructures (Equations (9) and (10)). The comparison with the first of Equations (20) suggests that in the first of Equations (10) the off-diagonal term $\mathbf{m}_{\mathrm{SP}}$ in the modal inertia matrix, $\mathbf{m}$, is proportional to the square root of the mass

ratio, $\sqrt{\alpha}$ (which is not negligible), while the increment $\Delta\mathbf{m}_{\mathrm{P}}$ is proportional to the mass ratio, α (which is negligible). Accordingly, the inverse of the matrix $\mathbf{m}$ for the multi-DOF P and S substructures can be approximated in a form similar to the one presented in Equation (25) for single-DOF P and S oscillators:

$$\hat{\mathbf{m}}^{-1} \cong \left[\begin{array}{c|c} \mathbf{I}_{m_{\mathrm{S}}} + \mathbf{m}_{\mathrm{SP}}\mathbf{m}_{\mathrm{SP}}^{T} & -\mathbf{m}_{\mathrm{SP}} \\ \hline -\mathbf{m}_{\mathrm{SP}}^{T} & \mathbf{I}_{m_{\mathrm{P}}} \end{array}\right] \tag{30}$$

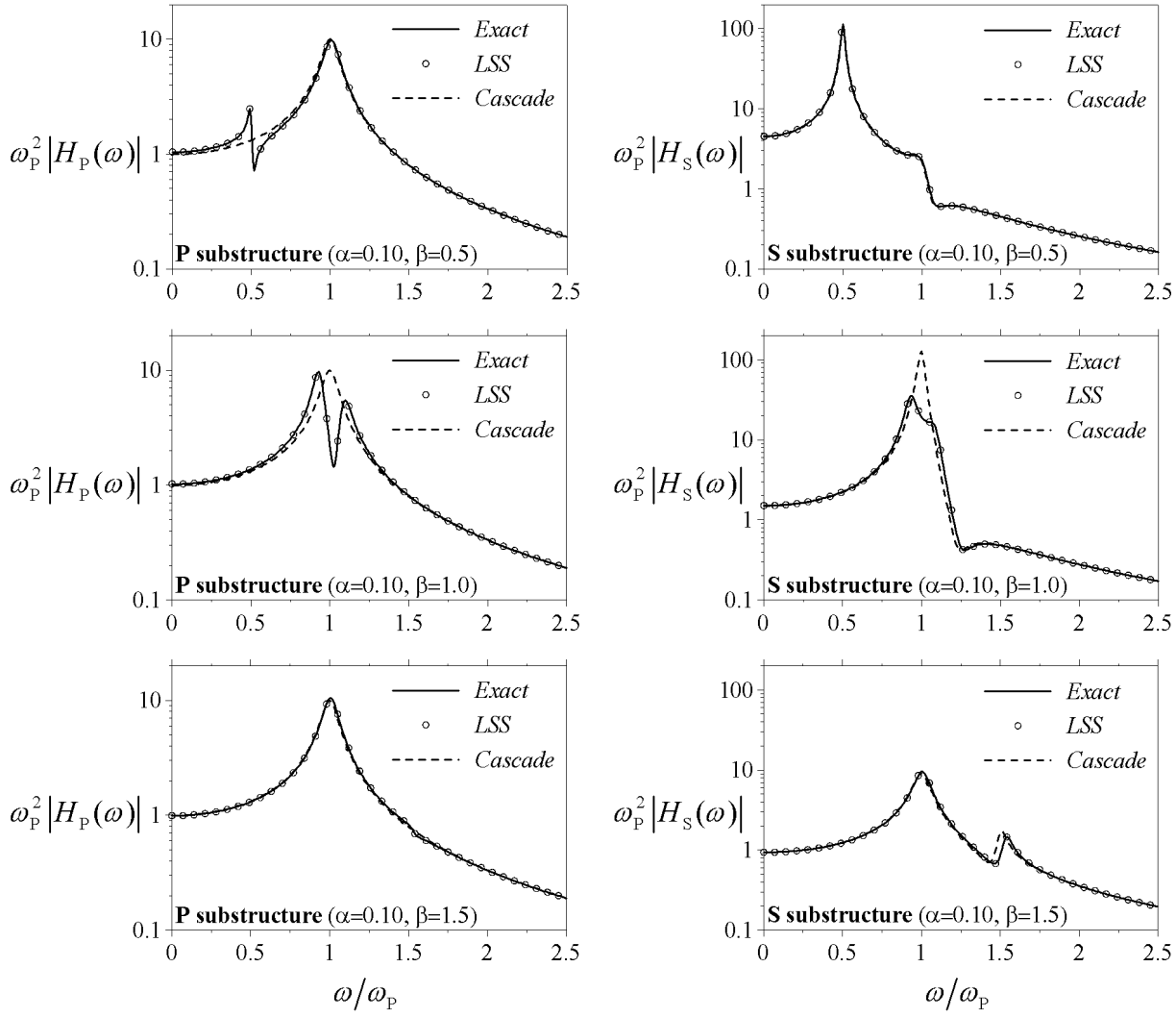

Fig. 6 Dimensionless absolute values of the frequency response functions of the 2-DOF combined P-S system with mass ratio $\alpha = 0.10$ and tuning parameter $\beta = 0.5$, 1.0 and 1.5: P oscillator (left); S oscillator (right)

Following the above approach, the dynamic stiffness matrix and the influence vector also take approximate forms similar to those derived in the case of single-DOF P and S oscillators (Equation (23)):

$$\hat{\mathbf{k}}(\omega) = \left[\begin{array}{c|c} \mathbf{\Omega}_{\mathrm{S}}^2\gamma(\omega) & \mathbf{0} \\ \hline \mathbf{0} & \mathbf{\Omega}_{\mathrm{P}}^2 \end{array}\right] \times \left[1 + \mathrm{j}\,\eta_{\mathrm{P}}\,\mathrm{sign}(\omega)\right]; \quad \hat{\mathbf{g}} = -\left[\begin{array}{c} \mathbf{p}_{\mathrm{S}} \\ \hline \mathbf{p}_{\mathrm{P}} \end{array}\right] \tag{31}$$

Then, substitution of Equations (30) and (31) into Equation (17) gives expressions similar to those of Equation (24):

$$\hat{\mathbf{A}}(\omega)=\hat{\mathbf{m}}^{-1}\hat{\mathbf{k}}(\omega)=\left[\begin{array}{c|c}\left(\mathbf{I}_{m_S}+\mathbf{m}_{SP}\mathbf{m}_{SP}^T\right)\boldsymbol{\Omega}_S^2\gamma(\omega) & -\mathbf{m}_{SP}\boldsymbol{\Omega}_P^2\\ \hline -\mathbf{m}_{SP}^T\boldsymbol{\Omega}_S^2\gamma(\omega) & \boldsymbol{\Omega}_P^2\end{array}\right]\times\left[1+\mathrm{j}\,\eta_P\,\mathrm{sign}(\omega)\right]$$
$$\hat{\mathbf{b}}=\hat{\mathbf{m}}^{-1}\hat{\mathbf{g}}=-\left[\begin{array}{c}\mathbf{p}_S-\mathbf{m}_{SP}\mathbf{p}_P\\ \hline \mathbf{p}_P\end{array}\right] \tag{32}$$

Moreover, substitution of Equation (32) into Equation (26) gives the array of the modal FRFs in the form,

$$\hat{\mathbf{h}}(\omega)=-\left\{\left[\begin{array}{c|c}\hat{\mathbf{A}}_S\gamma(\omega) & \hat{\mathbf{A}}_{SP}\\ \hline \hat{\mathbf{A}}_{PS}\gamma(\omega) & \boldsymbol{\Omega}_P^2\end{array}\right]\times\left[1+\mathrm{j}\,\eta_P\,\mathrm{sign}(\omega)\right]-\omega^2\left[\begin{array}{c|c}\mathbf{I}_{m_S} & \mathbf{0}\\ \hline \mathbf{0} & \mathbf{I}_{m_P}\end{array}\right]\right\}^{-1}\left[\begin{array}{c}\hat{\mathbf{b}}_S\\ \hline \mathbf{p}_P\end{array}\right] \tag{33}$$

with $\hat{\mathbf{A}}_S=\left(\mathbf{I}_{m_S}+\mathbf{m}_{SP}\mathbf{m}_{SP}^T\right)\boldsymbol{\Omega}_S^2$, $\hat{\mathbf{A}}_{SP}=-\mathbf{m}_{SP}\boldsymbol{\Omega}_P^2$, $\hat{\mathbf{A}}_{PS}=-\mathbf{m}_{SP}^T\boldsymbol{\Omega}_S^2$, and $\hat{\mathbf{b}}_S=\mathbf{p}_S-\mathbf{m}_{SP}\mathbf{p}_P$. Interestingly, in Equation (33) only the direct terms of the P substructure, namely the squared spectral matrix, $\boldsymbol{\Omega}_P^2$, and the array of the modal participation factors, $\mathbf{p}_P$, are unmodified by the coupling matrix $\mathbf{m}_{SP}$. Finally, once the array of Equation (33) is partitioned as $\hat{\mathbf{h}}(\omega)=\left[\hat{\mathbf{h}}_S^T(\omega)\;\middle|\;\hat{\mathbf{h}}_P^T(\omega)\right]^T$, the FRFs of various DOFs can be written similar to Equation (27):

$$\hat{\mathbf{H}}(\omega)=\boldsymbol{\Gamma}\hat{\mathbf{h}}(\omega)=\left[\begin{array}{c}\boldsymbol{\Phi}_S\hat{\mathbf{h}}_S(\omega)+\boldsymbol{\Psi}_{SP}\hat{\mathbf{h}}_P(\omega)\\ \hline \boldsymbol{\Phi}_P\hat{\mathbf{h}}_P(\omega)\end{array}\right] \tag{34}$$

MAXIMUM SECONDARY RESPONSE BY EARTHQUAKE RESPONSE SPECTRUM

The aim of this section is to derive a novel definition of the cross-correlation coefficients $\rho(i,k)$ that would enable the Complete Quadratic Combination (CQC) rule (Wilson et al., 1981) to be extended to the seismic analysis and design of multi-DOF secondary (S) substructures attached to a multi-DOF primary (P) load-bearing substructure. It is worth noting that, in order to be attractive for practical applications, (i) the proposed combination rule takes advantage of the LSS (light secondary substructure) approximation presented in the previous sections, and operates without evaluating the eigenproperties of the combined P-S system, while (ii) the seismic input is represented through a conventional earthquake response spectrum. Following the idea of Falsone and Muscolino (1999, 2004), the proposed cross-correlation coefficients would incorporate the dynamic effects which complicate the seismic response of S substructures with respect to the conventional fixed-base structures with equal viscous damping ratio in all the modes of vibration.

1. Preliminary Expressions

Let $y_S(t)$ be a generic response of interest (e.g., an internal force or a deformation measure) for the S attachment as well as for the P-S anchors. Owing to the linearity of both P and S substructures, $y_S(t)$ can be expressed as linear combination of the modal coordinates of the coupled P-S system:

$$\begin{aligned}y_S(t)&=\mathbf{E}_{SS}^T\mathbf{u}_S(t)+\mathbf{E}_{SP}^T\mathbf{u}_P(t)=\mathbf{E}_{SS}^T\boldsymbol{\Phi}_S\mathbf{q}_S(t)+\left(\mathbf{E}_{SS}^T\boldsymbol{\Psi}_{SP}+\mathbf{E}_{SP}^T\boldsymbol{\Phi}_P\right)\mathbf{q}_P(t)\\&=\mathbf{e}_{SS}^T\mathbf{q}_S(t)+\mathbf{e}_{SP}^T\mathbf{q}_P(t)=\sum\nolimits_{i=1}^{m_S}e_{SSi}q_{Si}(t)+\sum\nolimits_{i=1}^{m_P}e_{SPi}q_{Pi}(t)\end{aligned} \tag{35}$$

where $\mathbf{E}_{SS}$ (of dimensions $n_S\times 1$) and $\mathbf{E}_{SP}$ (of dimensions $n_P\times 1$) are the arrays listing the contributing coefficients for the DOFs, while the corresponding ones for the modal coordinates are given by $\mathbf{e}_{SS}=\boldsymbol{\Phi}_S^T\mathbf{E}_S$ (of dimensions $m_S\times 1$) and $\mathbf{e}_{SP}=\boldsymbol{\Phi}_P^T\mathbf{E}_{SP}+\boldsymbol{\Psi}_{SP}^T\mathbf{E}_{SS}$ (of dimensions $m_P\times 1$). According to the CQC rule (Wilson et al., 1981), the maximum seismic response can be computed as

$$\begin{aligned}\max\left|y_{\mathrm{S}}(t)\right| = \Big[& \sum_{i=1}^{m_{\mathrm{S}}}\sum_{k=1}^{m_{\mathrm{S}}} \rho_{\mathrm{SS}}(i,k) e_{\mathrm{SS}i} e_{\mathrm{SS}k} \max\left|q_{\mathrm{S}i}(t)\right| \max\left|q_{\mathrm{S}k}(t)\right| \\ & + \sum_{i=1}^{m_{\mathrm{P}}}\sum_{k=1}^{m_{\mathrm{P}}} \rho_{\mathrm{PP}}(i,k) e_{\mathrm{SP}i} e_{\mathrm{SP}k} \max\left|q_{\mathrm{P}i}(t)\right| \max\left|q_{\mathrm{P}k}(t)\right| \\ & + 2\sum_{i=1}^{m_{\mathrm{S}}}\sum_{k=1}^{m_{\mathrm{P}}} \rho_{\mathrm{SP}}(i,k) e_{\mathrm{SS}i} e_{\mathrm{SP}k} \max\left|q_{\mathrm{S}i}(t)\right| \max\left|q_{\mathrm{P}k}(t)\right| \Big]^{1/2}\end{aligned} \tag{36}$$

Here $\rho_{\mathrm{AB}}(i,k)$ stands for the cross-correlation coefficient among the ith modal coordinate of the A substructure, $q_{\mathrm{A}i}(t)$, and the kth modal coordinate of the B substructure, $q_{\mathrm{B}k}(t)$, with A = P, S, B = P, S, $i = 1,...,m_{\mathrm{A}}$ and $k = 1,...,m_{\mathrm{B}}$:

$$\rho_{\mathrm{AB}}(i,k) = \frac{\mathrm{E}\left\langle q_{\mathrm{A}i}(t) q_{\mathrm{B}k}(t)\right\rangle}{\sqrt{\mathrm{E}\left\langle q_{\mathrm{A}i}^2(t)\right\rangle \mathrm{E}\left\langle q_{\mathrm{B}k}^2(t)\right\rangle}} \tag{37}$$

In Equation (37), $\mathrm{E}\langle\cdot\rangle$ denotes the expectation operator. The cross-correlation coefficients are usually evaluated under the assumption that the seismic acceleration is a zero-mean, stationary, Gaussian process, which can be modelled as white noise (Der Kiureghian, 1981), filtered white noise (Der Kiureghian and Nakamura, 1993), or spectrum-compatible coloured process (Cacciola et al., 2004). Moreover, it should be emphasized that the CQC rule has been originally derived under the assumption that the peak factor, PF, of the structural response of interest, $y(t)$, is approximately equal to the peak factors of the contributing modal coordinates, $q_i(t)$, i.e.,

$$PF = \frac{\max\left|y(t)\right|}{\sqrt{\mathrm{E}\left\langle y^2(t)\right\rangle}} = \frac{\max\left|q_i(t)\right|}{\sqrt{\mathrm{E}\left\langle q_i^2(t)\right\rangle}} \tag{38}$$

2. Proposed Cross-Correlation Coefficients

Let us now rewrite Equation (37) in the equivalent form:

$$\rho_{\mathrm{AB}}(i,k) = r_{\mathrm{AB}}(i,k) \frac{\hat{b}_{\mathrm{A}i}\hat{b}_{\mathrm{B}k}\sigma_{\mathrm{A}i}\sigma_{\mathrm{B}k}}{\sqrt{\mathrm{E}\left\langle q_{\mathrm{A}i}^2(t)\right\rangle}\sqrt{\mathrm{E}\left\langle q_{\mathrm{B}k}^2(t)\right\rangle}} \tag{39}$$

where

$$r_{\mathrm{AB}}(i,k) = \frac{\mathrm{E}\left\langle q_{\mathrm{A}i}(t) q_{\mathrm{B}k}(t)\right\rangle}{\left(\hat{b}_{\mathrm{A}i}\sigma_{\mathrm{A}i}\right)\left(\hat{b}_{\mathrm{B}k}\sigma_{\mathrm{B}k}\right)} \tag{40}$$

Here, $\sigma_{\mathrm{A}i}$ and $\sigma_{\mathrm{B}k}$ are the standard deviations of the stationary seismic response of auxiliary single-DOF oscillators having unit mass, a reference value of the viscous damping ratio, ζ_{ref}, for which the earthquake response spectrum is known (usually, $\zeta_{\mathrm{ref}} = 0.05$), and undamped natural periods of the decoupled A and B substructures, respectively. For instance, the undamped natural period of the Aith auxiliary oscillator is

$$T_{\mathrm{A}i} = \frac{2\pi}{\omega_{\mathrm{A}i}} \quad (\mathrm{A} = \mathrm{P},\ \mathrm{S};\ i = 1,...,m_{\mathrm{A}}) \tag{41}$$

Further, according to the second of Equations (32), the coefficient $\hat{b}_{\mathrm{A}i}$ in Equations (39) and (40) plays the role of modal participation factors, and is expressed for the P and S substructures as

$$\hat{b}_{\mathrm{A}i} = \begin{cases} -p_{\mathrm{P}i}; & \mathrm{A} = \mathrm{P} \\ -p_{\mathrm{S}i} + \boldsymbol{\phi}_{\mathrm{S}i}^T \sum_{k=1}^{m_{\mathrm{P}}} p_{\mathrm{P}k} \mathbf{M}_{\mathrm{S}} \boldsymbol{\psi}_{\mathrm{SP}k}; & \mathrm{A} = \mathrm{S} \end{cases} \tag{42}$$

In other words, for the P substructure the coefficients $\hat{b}_{\mathrm{P}i}$ are the modal participation factors $p_{\mathrm{P}i}$, evaluated without considering the presence of attachments (as in second of Equations (12)), while for the S substructure the coefficients $\hat{b}_{\mathrm{S}i}$ are given by the modal participation factors $p_{\mathrm{S}i}$ of the fixed-base attachment (as in first of Equation (12)), appropriately modified by the interaction with the P structural system.

As a result of the above definitions, the product $\left(\hat{b}_{\mathrm{A}i}\sigma_{\mathrm{A}i}\right)$ in Equation (40) is the standard deviation of the steady-state response of a classical single-DOF oscillator governed by

$$\ddot{q}_{\mathrm{A}i}^{(0)}(t)+2\zeta_{\mathrm{ref}}\omega_{\mathrm{A}i}\dot{q}_{\mathrm{A}i}^{(0)}(t)+\omega_{\mathrm{A}i}^{2}q_{\mathrm{A}i}^{(0)}(t)=\hat{b}_{\mathrm{A}i}\ddot{u}_{\mathrm{g}}(t) \tag{43}$$

Under the assumption that the ground acceleration is a white noise of unit one-sided power spectral density, this quantity is expressed in closed-form as

$$\left(\hat{b}_{\mathrm{A}i}\sigma_{\mathrm{A}i}\right)=\sqrt{\mathrm{E}\left\langle\left[q_{\mathrm{A}i}^{(0)}(t)\right]^{2}\right\rangle}=\frac{1}{2}\sqrt{\frac{\pi}{\zeta_{\mathrm{ref}}\omega_{\mathrm{A}i}^{3}}} \tag{44}$$

On the other hand, the expectation in the numerator of Equation (40) can be evaluated in the frequency domain through the numerical integral:

$$\mathrm{E}\left\langle q_{\mathrm{A}i}(t)q_{\mathrm{B}k}(t)\right\rangle=\int_{0}^{\omega_{\mathrm{c}}}\hat{h}_{\mathrm{A}i}(\omega)\hat{h}_{\mathrm{B}k}^{*}(\omega)\mathrm{d}\omega \tag{45}$$

where ω_{c} is the cut-off circular frequency, and the superscripted asterisk means complex conjugate. Further, $\hat{h}_{\mathrm{A}i}(\omega)$ and $\hat{h}_{\mathrm{B}k}(\omega)$ are the approximate complex-valued FRFs of the modal coordinates $q_{\mathrm{A}i}(t)$ and $q_{\mathrm{B}k}(t)$, given by the *i*th element of $\hat{\mathbf{h}}_{\mathrm{A}}(\omega)$ and the *k*th element of $\hat{\mathbf{h}}_{\mathrm{B}}(\omega)$, respectively. It is worth noting that the assumption of white noise input, although effective in a number of real circumstances, should be carefully checked in the cases of soft soil and/or stiff structural system (Der Kiureghian and Nakamura, 1993; Cacciola et al., 2004; Palmeri, 2006). Since the proposed cross-correlation coefficients are evaluated in the frequency domain, the effects of a non-white input can be easily included.

The new coefficients $r_{\mathrm{AB}}(i,k)$ defined in Equation (40) can be evaluated by using Equations (44) and (45), and thus, each term in the double summations of Equation (36) can be written as

$$\rho_{\mathrm{AB}}(i,k)\max\left|q_{\mathrm{A}i}(t)\right|\max\left|q_{\mathrm{B}k}(t)\right|=r_{\mathrm{AB}}(i,k)\left[\frac{\hat{b}_{\mathrm{A}i}\sigma_{\mathrm{A}i}\max\left|q_{\mathrm{A}i}(t)\right|}{\sqrt{\mathrm{E}\left\langle q_{\mathrm{A}i}^{2}(t)\right\rangle}}\right]\left[\frac{\hat{b}_{\mathrm{B}k}\sigma_{\mathrm{B}k}\max\left|q_{\mathrm{B}k}(t)\right|}{\sqrt{\mathrm{E}\left\langle q_{\mathrm{B}k}^{2}(t)\right\rangle}}\right] \tag{46}$$

Taking into account Equation (38), this expression can be approximated as

$$\rho_{\mathrm{AB}}(i,k)\max\left|q_{\mathrm{A}i}(t)\right|\max\left|q_{\mathrm{B}k}(t)\right|=r_{\mathrm{AB}}(i,k)\hat{b}_{\mathrm{A}i}\hat{b}_{\mathrm{B}k}\left[\sigma_{Ai}PF\right]\left[\sigma_{Bk}PF\right] \tag{47}$$

Further, the terms $\left[\sigma_{\mathrm{A}i}PF\right]$ and $\left[\sigma_{\mathrm{B}k}PF\right]$ can be viewed as the maximum seismic responses of the auxiliary single-DOF oscillators with undamped natural periods $T_{\mathrm{A}i}$ and $T_{\mathrm{B}k}$, respectively, and therefore, the previous expression can be rewritten as

$$\rho_{\mathrm{AB}}(i,k)\max\left|q_{\mathrm{A}i}(t)\right|\max\left|q_{\mathrm{B}k}(t)\right|=r_{\mathrm{AB}}(i,k)\hat{b}_{\mathrm{A}i}\hat{b}_{\mathrm{B}k}\frac{S_{\mathrm{a}}\left(T_{\mathrm{A}i},\zeta_{\mathrm{ref}}\right)}{\left(2\pi/T_{\mathrm{A}i}\right)^{2}}\frac{S_{\mathrm{a}}\left(T_{\mathrm{B}k},\zeta_{\mathrm{ref}}\right)}{\left(2\pi/T_{\mathrm{B}k}\right)^{2}} \tag{48}$$

Here $S_{\mathrm{a}}\left(T,\zeta\right)$ denotes the earthquake response spectrum in terms of pseudo-acceleration for undamped natural period T and viscous damping ratio ζ, and the coefficients $r_{\mathrm{AB}}(i,k)$ are obtained by substituting Equation (44) into Equation (40):

$$r_{\mathrm{AB}}(i,k)=\frac{4\zeta_{\mathrm{ref}}}{\pi}\omega_{\mathrm{A}i}\omega_{\mathrm{B}k}\sqrt{\omega_{\mathrm{A}i}\omega_{\mathrm{B}k}}\,\mathrm{E}\left\langle q_{\mathrm{A}i}(t)q_{\mathrm{B}k}(t)\right\rangle \tag{49}$$

In Equation (49) only the expectation of Equation (45) has to be computed. Finally, upon substitution of Equation (48) into Equation (36), one obtains the CQC rule for the response of interest:

$$\begin{aligned}\max\left|y_{\mathrm{S}}(t)\right| = \frac{1}{4\pi^2}\Big[&\sum_{i=1}^{m_{\mathrm{S}}}\sum_{k=1}^{m_{\mathrm{S}}} r_{\mathrm{SS}}(i,k)e_{\mathrm{SS}i}e_{\mathrm{SS}k}\hat{b}_{\mathrm{S}i}\hat{b}_{\mathrm{S}k}T_{\mathrm{S}i}^2T_{\mathrm{S}k}^2 S_{\mathrm{a}}\left(T_{\mathrm{S}i},\zeta_{\mathrm{ref}}\right)S_{\mathrm{a}}\left(T_{\mathrm{S}k},\zeta_{\mathrm{ref}}\right)\\ &+\sum_{i=1}^{m_{\mathrm{P}}}\sum_{k=1}^{m_{\mathrm{P}}} r_{\mathrm{PP}}(i,k)e_{\mathrm{SP}i}e_{\mathrm{SP}k}\hat{b}_{\mathrm{P}i}\hat{b}_{\mathrm{P}k}T_{\mathrm{P}i}^2T_{\mathrm{P}k}^2 S_{\mathrm{a}}\left(T_{\mathrm{P}i},\zeta_{\mathrm{ref}}\right)S_{\mathrm{a}}\left(T_{\mathrm{P}k},\zeta_{\mathrm{ref}}\right)\\ &+2\sum_{i=1}^{m_{\mathrm{S}}}\sum_{k=1}^{m_{\mathrm{P}}} r_{\mathrm{SP}}(i,k)e_{\mathrm{SS}i}e_{\mathrm{SP}k}\hat{b}_{\mathrm{S}i}\hat{b}_{\mathrm{P}k}T_{\mathrm{S}i}^2T_{\mathrm{P}k}^2 S_{\mathrm{a}}\left(T_{\mathrm{S}i},\zeta_{\mathrm{ref}}\right)S_{\mathrm{a}}\left(T_{\mathrm{P}k},\zeta_{\mathrm{ref}}\right)\Big]^{1/2}\end{aligned} \tag{50}$$

NUMERICAL APPLICATION

The CQC rule proposed in the previous section has been applied to the 6-DOF P-S system shown in Figure 7. The P substructure is a planar shear-type 3-DOF frame, with storey mass $M_{\mathrm{P}} = 3{,}000\ \mathrm{kg}$ and storey stiffness $K_{\mathrm{P}} = 3{,}000\ \mathrm{kN/m}$, while the loss coefficient is $\eta_{\mathrm{P}} = 0.10$ (the equivalent viscous damping ratio is $\zeta_{\mathrm{P}} = \eta_{\mathrm{P}}/2 = 0.05$). The S substructure is a 3-DOF attachment, with lumped mass $M_{\mathrm{S}} = \alpha M_{\mathrm{P}}$, lumped stiffness $K_{\mathrm{S}} = 889\,\alpha\beta^2\ \mathrm{kN/m}$, and anchor stiffness $K_{\mathrm{SP}} = 1{,}207\,\alpha\beta^2\ \mathrm{kN/m}$ (the dimensionless variables α and β being the mass ratio and tuning parameter, respectively), while the loss coefficient is $\eta_{\mathrm{S}} = 0.04$ (equivalent viscous damping ratio $\zeta_{\mathrm{S}} = 0.02$). The undamped modal circular frequencies of the fixed-base substructures, i.e., solutions of the eigenproblems given in Equation (7), are $\omega_{\mathrm{P}1} = 16.4$, $\omega_{\mathrm{P}2} = 44.7$ and $\omega_{\mathrm{P}3} = 61.1\ \mathrm{rad/s}$ for the P frame, and $\omega_{\mathrm{S}1} = 16.4\beta$, $\omega_{\mathrm{S}2} = 28.6\beta$ and $\omega_{\mathrm{S}3} = 34.6\beta\ \mathrm{rad/s}$ for the S attachment.

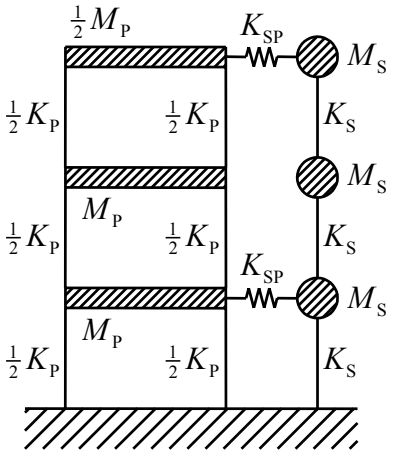

Fig. 7 Combined P frame-S attachment under investigation

When the coupled P-S system is considered, the undamped modal circular frequencies, ω_i, and the corresponding viscous damping ratios, ζ_i (with $i = 1, \ldots, 6$), strongly depend on mass ratio and tuning parameter. For comparison, the values of ω_i (in $\mathrm{rad/s}$) and of ζ_i, given by the modal strain energy (Johnson and Kienholz, 1982), are listed in Table 1 for $\alpha = 0.05$ and $\beta = 0.50$, 1.00, and 1.50. Interestingly, all the computed viscous damping ratios are in the range $0.02 \le \zeta_i \le 0.05$, and those take values close to $\zeta_{\mathrm{P}} = 0.05$ or to $\zeta_{\mathrm{S}} = 0.02$ when the corresponding modal shapes resemble those of the P frame or of the S attachment, respectively. On the contrary, intermediate values of the viscous damping ratio indicate coupling between the fixed-base modal shapes of P and S substructures (e.g., ω_1 and ω_2 for $\beta = 1.00$; ω_3 and ω_4 for $\beta = 1.50$).

The reference earthquake response spectrum for the viscous damping ratio $\zeta_{\text{ref}} = 0.05$ (Figure 8, thick line) has been defined by averaging the spectra of eight recorded accelerograms (Figure 8, thin lines) normalized with respect to the peak ground acceleration, *PGA*. These accelerograms, depicted in Figure 9, are the orthogonal components of the four strong ground motions chronologically listed in Table 2 (PEER Strong Motion Database[1]).

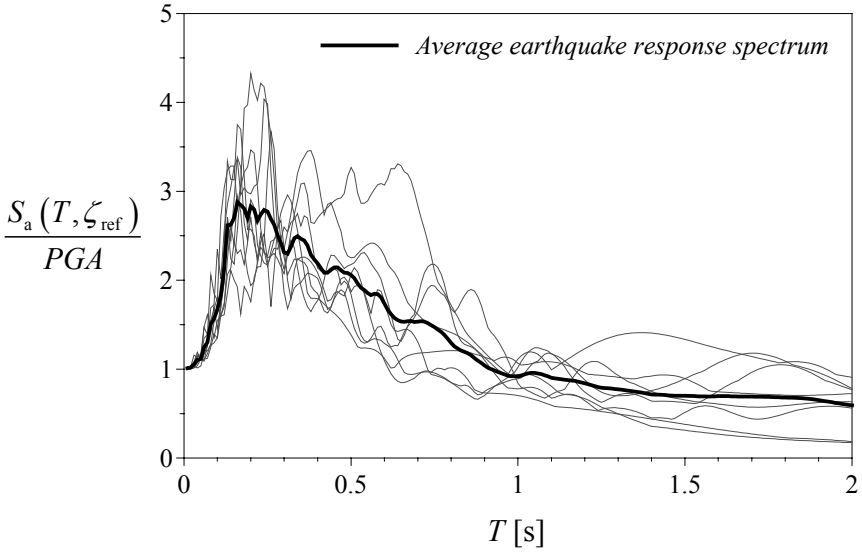

Fig. 8 Normalized response spectra for the recorded accelerograms listed in Table 2 (thin lines) and average earthquake response spectrum (thick line)

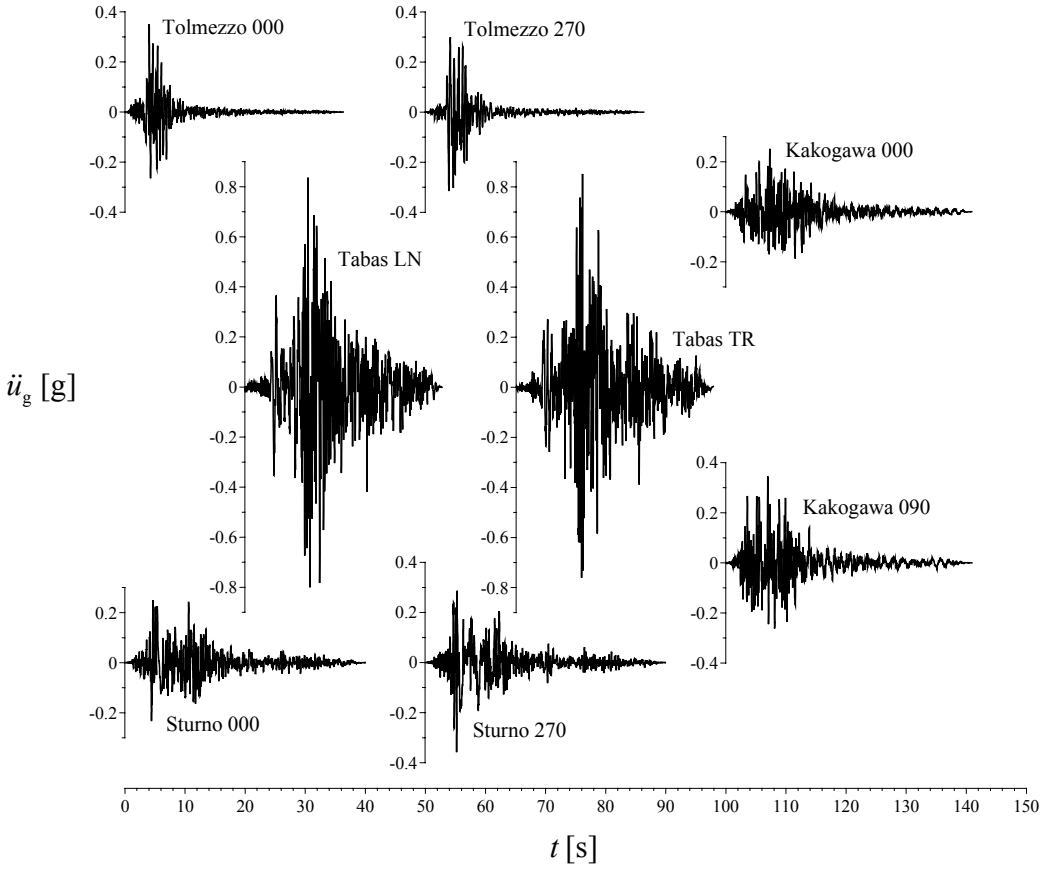

Fig. 9 Recorded accelerograms listed in Table 2

[1] Website of PEER Strong Motion Database, http://peer.berkeley.edu/smcat/

Table 1: Undamped Natural Frequencies (in rad/s) and Viscous Damping Ratios of the Combined P-S System Depicted in Figure 7 for Mass Ratio $\alpha = 0.05$ and Tuning Parameter $\beta = 0.50$, 1.00 and 1.50

$\alpha = 0.05, \beta = 0.50$		$\alpha = 0.05, \beta = 1.00$		$\alpha = 0.05, \beta = 1.50$	
$\omega_1 = 8.13$	$\zeta_1 = 0.0205$	$\omega_1 = 14.9$	$\zeta_1 = 0.0359$	$\omega_1 = 16.0$	$\zeta_1 = 0.0480$
$\omega_2 = 14.3$	$\zeta_2 = 0.0208$	$\omega_2 = 18.0$	$\zeta_2 = 0.0338$	$\omega_2 = 25.2$	$\zeta_2 = 0.0216$
$\omega_3 = 16.4$	$\zeta_3 = 0.0449$	$\omega_3 = 28.5$	$\zeta_3 = 0.0205$	$\omega_3 = 41.3$	$\zeta_3 = 0.0300$
$\omega_4 = 17.5$	$\zeta_4 = 0.0239$	$\omega_4 = 34.6$	$\zeta_4 = 0.0201$	$\omega_4 = 46.8$	$\zeta_4 = 0.0393$
$\omega_5 = 44.8$	$\zeta_5 = 0.0499$	$\omega_5 = 45.1$	$\zeta_5 = 0.0492$	$\omega_5 = 52.0$	$\zeta_5 = 0.0208$
$\omega_6 = 61.1$	$\zeta_6 = 0.0500$	$\omega_6 = 61.2$	$\zeta_6 = 0.0498$	$\omega_6 = 61.6$	$\zeta_6 = 0.0491$

Table 2: Information Pertinent to the Strong Motions Selected in This Study

Earthquake, Date	M, Ml	Station	Component	PGA (*g*)	PGV (cm/s)	PGD (cm)
Friuli, Italy, May 6, 1976	6.5, 6.2	Tolmezzo	000	0.351	22.0	4.1
			270	0.315	30.8	5.1
Tabas, Iran, September 16, 1978	7.4, 7.7	Tabas	LN	0.836	97.8	36.92
			TR	0.852	121.4	94.58
Irpinia, Italy, November 23, 1980	–, 6.5	Sturno	000	0.251	37.0	11.77
			270	0.358	52.7	33.08
Kobe, Japan, January 16, 1995	6.9, –	Kakogawa	000	0.251	18.7	5.83
			090	0.345	27.6	9.6

The average drifts in the S attachment, i.e., the mean value of the strains in the secondary springs k_S (as in Figure 7), and the average deformations in the P-S anchors, i.e., the mean value of the strains in the primary-secondary springs k_{SP} (as in Figure 7), have been selected as seismic responses of interest. Two values of the mass ratio, $\alpha = 0.01$ and 0.05, have been considered. Only the first mode has been retained for the P frame ($m_P = 1$, modal participating mass = 92.3%) in the proposed CQC rule (as in Equation (50)), while two modes have been retained for the S attachment ($m_S = 2$, modal participating mass = 89.5%). Figure 10 shows the percentage error ε as function of the tuning parameter in the range $0.5 \le \beta \le 2.0$, assuming that the "exact" values are the respective average maxima given by the eight time-history analyses. The accuracy of the proposed approach (shown by the solid line) proves to be very good from an engineering point of view. More precisely, in the case of "soft" attachments ($0.5 \le \beta \le 1.2$) the results are slightly conservative ($0 < \varepsilon < 25\%$), while for the "stiff" attachments ($1.2 \le \beta \le 2.0$) the seismic demand is slightly underestimated ($-25 < \varepsilon < 0\%$). A couple of considerations would confirm the effectiveness of the proposed method: (i) the numerical test is extremely severe, since the analyses are carried out not with stochastically generated accelerograms, but with recorded accelerograms, having quite different time-frequency characteristics; and (ii) the level of confidence is similar to that of the original CQC rule for the classically damped structures. On the contrary, a conventional analysis with the earthquake response spectrum based on the cascade approximation (shown by the dashed lines) proves to be absolutely inadequate: the seismic response of soft attachments, in fact, is heavily underestimated, since the percentage error may be as low as -100%; conversely, the results for the anchors of stiff attachment are excessively conservative, since the percentage error may be larger than 100%. It is worth noting that according to the current Italian seismic code (PCM, 2003), the conventional response of the S attachment is evaluated as the quasi-static response to the seismic motion of the P frame. More precisely, in this (cascade) approximation, the maximum seismic response, $\max|y_S(t)|$, is still given by Equation (36) in which the coefficients $\rho_{SS}(i,k)$ and

$\rho_{SP}(i,k)$ go to zero and in which $\rho_{PP}(i,k)$ is the cross-correlation coefficient proposed by Der Kiureghian (1981).

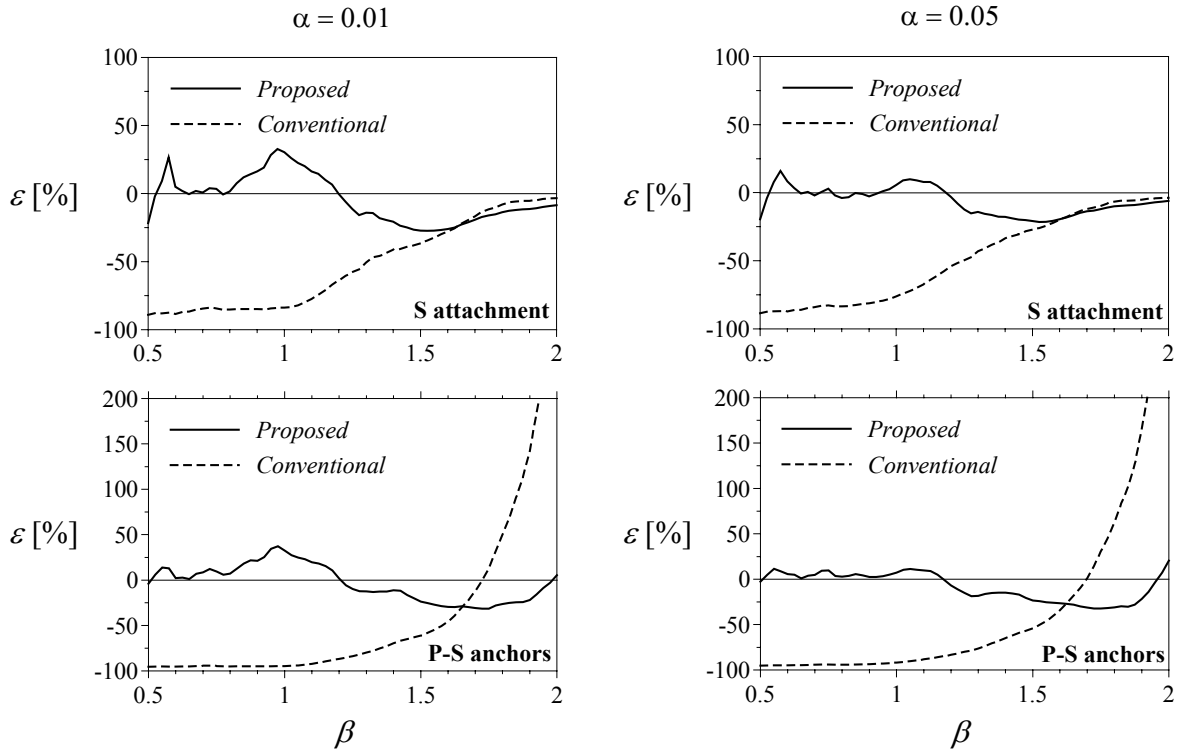

Fig. 10 Comparison between the proposed (solid lines) and conventional (dashed lines) CQC rules for the S attachment (top) and the P-S anchors (bottom); tuning parameter in the range $0.5 \le \beta \le 2.0$; mass ratios $\alpha = 0.01$ (left) and 0.05 (right)

CONCLUSIONS

In this paper, a novel Complete Quadratic Combination (CQC) rule for the seismic analysis and design of multi-DOF secondary (S) attachments to multi-DOF primary (P) structural systems has been proposed and numerically validated. In the first stage, in contrast with the classical "cascade" approximation, which neglects the feedback of the S substructure to the P substructure, the accuracy of the "Light Secondary Substructure" (LSS) approximation has been proved. In the second stage, the latter approximation has been used in evaluating the cross-correlation coefficients in the CQC rule. These coefficients are quite different from those available in the literature, since they would directly include, in the combination rule, the effects of frequency tuning among P and S frequencies and different damping ratios in the components. For the purpose of validation, the results of a severe numerical investigation, with eight recorded accelerograms, have been presented and discussed.

Two main features make the proposed method particularly attractive for practical analyses: (i) modal frequencies and modal shapes used in the combination rule are those of the decoupled substructures, assumed to be fixed to their own bases, i.e., the eigenproperties of the combined P-S system are not required; and (ii) the earthquake response spectrum for only a single value of the viscous damping ratio is used, and this reference value can be different from the viscous damping ratios of the components.

Finally, it is worth noting that the cross-correlation coefficients have been derived in this paper under the restrictive assumptions that (i) the ground acceleration is a stationary white noise, and that (ii) the peak factors of the structural response of interest are equal to those of the contributing modal coordinates. More accurate results, therefore, can be obtained by removing these assumptions, even if at the same time the procedure would become cumbersome; these possible improvements will be the subject of future work.

REFERENCES

1. Amini, A. and Trifunac, M.D. (1985). "Statistical Extension of Response Spectrum Superposition", International Journal of Soil Dynamics and Earthquake Engineering, Vol. 4, No. 2, pp. 54–63.
2. Biot, M.A. (1932). "Transient Oscillations in Elastic Systems", Ph.D. Thesis No. 259, Aeronautics Department, California Institute of Technology, Pasadena, U.S.A.
3. Biot, M.A. (1933). "Theory of Elastic Systems Vibrating under Transient Impulse with an Application to Earthquake-Proof Buildings", Proceedings of the National Academy of Sciences of the United States of America, Vol. 19, No. 2, pp. 262–268.
4. Biot, M.A. (1934). "Theory of Vibration of Buildings during Earthquake", Zeitschrift für Angewandte Matematik und Mechanik, Vol. 14, No. 4, pp. 213–223.
5. Cacciola, P., Colajanni, P. and Muscolino, G. (2004). "Combination of Modal Responses Consistent with Seismic Input Representation", Journal of Structural Engineering, ASCE, Vol. 130, No. 1, pp. 47–55.
6. Chen, Y. and Soong, T.T. (1988). "State-of-the-Art Review: Seismic Response of Secondary Systems", Engineering Structures, Vol. 10, No. 4, pp. 218–228.
7. Der Kiureghian, A. (1981). "A Response Spectrum Method for Random Vibration Analysis of MDF systems," Earthquake Engineering & Structural Dynamics, Vol. 9, No. 5, pp. 419–435.
8. Der Kiureghian, A. and Nakamura, Y. (1993). "CQC Modal Combination Rule for High-Frequency Modes", Earthquake Engineering & Structural Dynamics, Vol. 22, No. 11, pp. 943–956.
9. Der Kiureghian, A. and Neuenhofer, A. (1992). "Response Spectrum Method for Multi-Support Seismic Excitations", Earthquake Engineering & Structural Dynamics, Vol. 21, No. 8, pp. 713–740.
10. Dey, A. and Gupta, V.K. (1999). "Stochastic Seismic Response of Multiply-Supported Secondary Systems in Flexible-Base Structures", Earthquake Engineering & Structural Dynamics, Vol. 28, No. 4, pp. 351–369.
11. Falsone, G. and Muscolino, G. (1999). "Cross-Correlation Coefficients and Modal Combination Rules for Non-classically Damped Systems", Earthquake Engineering & Structural Dynamics, Vol. 28, No. 12, pp. 1669–1684.
12. Falsone, G. and Muscolino, G. (2004). "New Real-Value Modal Combination Rules for Non-classically Damped Structures", Earthquake Engineering & Structural Dynamics, Vol. 33, No. 12, pp. 1187–1209.
13. Falsone, G., Muscolino, G. and Ricciardi, G. (1991). "Combined Dynamic Response of Primary and Multiply Connected Cascaded Secondary Subsystems", Earthquake Engineering & Structural Dynamics, Vol. 20, No. 8, pp. 749–767.
14. Feriani, A. and Perotti, F. (1996). "The Formation of Viscous Damping Matrices for the Dynamic Analysis of MDOF Systems", Earthquake Engineering & Structural Dynamics, Vol. 25, No. 7, pp. 689–709.
15. Gupta, A.K. and Jaw, J.W. (1986). "Seismic Response of Nonclassically Damped Systems", Nuclear Engineering and Design, Vol. 91, No. 2, pp. 153–159.
16. Gupta, I.D. and Trifunac, M.D. (1988). "Order Statistics of Peaks in Earthquake Response", Journal of Engineering Mechanics, ASCE, Vol. 114, No. 10, pp. 1605–1627.
17. Gupta, V.K. and Trifunac, M.D. (1989). "Investigation of Building Response to Translational and Rotational Earthquake Excitations", Report CE 89-02, University of Southern California, Los Angeles, U.S.A.
18. Inaudi, J.A. and Kelly, J.M. (1995). "Linear Hysteretic Damping and the Hilbert Transform", Journal of Engineering Mechanics, ASCE, Vol. 121, No. 5, pp. 626–632.
19. Iwan, W.D. (1997) "Drift Spectrum: Measure of Demand for Earthquake Ground Motions", Journal of Structural Engineering, ASCE, Vol. 123, No. 4, pp. 397–404.
20. Johnson, C.D. and Kienholz, D.A. (1982). "Finite Element Prediction of Damping in Structures with Constrained Viscoelastic Layers", AIAA Journal, Vol. 20, No. 9, pp. 1284–1290.

21. Lavelle, F.M., Bergman, L.A. and Spanos, P.D. (1991). "Seismic Response Spectra of a Combined System by Green's Functions", Soil Dynamics and Earthquake Engineering, Vol. 10, No. 2, pp. 93–100.
22. Makris, N. (1997). "Causal Hysteretic Element", Journal of Engineering Mechanics, ASCE, Vol. 123, No. 11, pp. 1209–1214.
23. Makris, N. and Zhang, J. (2000). "Time-Domain Viscoelastic Analysis of Earth Structures", Earthquake Engineering & Structural Dynamics, Vol. 29, No. 6, pp. 745–768.
24. Muscolino, G. (1990). "Dynamic Response of Multiply Connected Primary-Secondary Systems", Earthquake Engineering & Structural Dynamics, Vol. 19, No. 2, pp. 205–216.
25. Muscolino, G., Palmeri, A. and Ricciardelli, F. (2005). "Time-Domain Response of Linear Hysteretic Systems to Deterministic and Random Excitations", Earthquake Engineering & Structural Dynamics, Vol. 34, No. 9, pp. 1129–1147.
26. Nashif, A.D., Jones, D.I. and Henderson, J.P. (1985). "Vibration Damping", John Wiley & Sons, New York, U.S.A.
27. Palmeri, A. (2006). "Correlation Coefficients for Structures with Viscoelastic Dampers", Engineering Structures, Vol. 28, No. 8, pp. 1197–1208.
28. PCM (2003). "Ordinanza 3274: Primi Elementi in Materia di Criteri Generali per la Classificazione Sismica del Territorio Nazionale e di Normative Tecniche per le Costruzioni in Zona Sismica", Presidenza del Consiglio dei Ministri, Rome, Italy (in Italian).
29. Singh, M.P. (1988). "Seismic Design of Secondary Systems", Probabilistic Engineering Mechanics, Vol. 3, No. 3, pp. 151–158.
30. Singh, M.P., Moreschi, L.M., Suárez, L.E. and Matheu, E.E. (2006a). "Seismic Design Forces. I: Rigid Nonstructural Components", Journal of Structural Engineering, ASCE, Vol. 132, No. 10, pp. 1524–1532.
31. Singh, M.P., Moreschi, L.M., Suárez, L.E. and Matheu, E.E. (2006b). "Seismic Design Forces. II: Flexible Nonstructural Components", Journal of Structural Engineering, ASCE, Vol. 132, No. 10, pp. 1533–1542.
32. Villaverde, R. (2004). "Seismic Analysis and Design of Nonstructural Elements" in "Earthquake Engineering: From Engineering Seismology to Performance-Based Engineering (edited by Y. Bozorgnia and V.V. Bertero)", CRC Press, Boca Raton, U.S.A.
33. Wilson, E.L., Der Kiureghian, A. and Bayo, E.P. (1981). "A Replacement for the SRSS Method in Seismic Analysis", Earthquake Engineering & Structural Dynamics, Vol. 9, No. 2, pp. 187–192.